



# Reductive nitrosylation of ferric human hemoglobin bound to human haptoglobin 1-1 and 2-2

Paolo Ascenzi<sup>1</sup> · Giovanna De Simone<sup>2</sup> · Fabio Polticelli<sup>2,3</sup> · Magda Gioia<sup>4,5</sup> · Massimo Coletta<sup>4,5</sup>

Received: 14 December 2017 / Accepted: 9 March 2018 / Published online: 31 March 2018  
© SBIC 2018

## Abstract

Haptoglobin (Hp) sequesters hemoglobin (Hb) preventing the Hb-based damage occurring upon its physiological release into plasma. Here, reductive nitrosylation of ferric human hemoglobin [Hb(III)] bound to human haptoglobin (Hp) 1-1 and 2-2 [Hp1-1:Hb(III) and Hp2-2:Hb(III), respectively] has been investigated between pH 7.5 and 9.5, at  $T=20.0$  °C. Over the whole pH range explored, only one process is detected reflecting NO binding to Hp1-1:Hb(III) and Hp2-2:Hb(III). Values of the pseudo-first-order rate constant for Hp1-1:Hb(III) and Hp2-2:Hb(III) nitrosylation ( $k$ ) do not depend linearly on the ligand concentration but tend to level off. The conversion of Hp1-1:Hb(III)-NO to Hp1-1:Hb(II)-NO and of Hp2-2:Hb(III)-NO to Hp2-2:Hb(II)-NO is limited by the OH<sup>-</sup> and H<sub>2</sub>O-based catalysis. In fact, bimolecular NO binding to Hp1-1:Hb(III), Hp2-2:Hb(III), Hp1-1:Hb(II), and Hp2-2:Hb(II) proceeds very rapidly. The analysis of data allowed to determine the values of the dissociation equilibrium constant for Hp1-1:Hb(III) and Hp2-2:Hb(III) nitrosylation [ $K = (1.2 \pm 0.1) \times 10^{-4}$  M], which is pH-independent, and of the first-order rate constant for Hp1-1:Hb(III) and Hp2-2:Hb(III) conversion to Hp1-1:Hb(II)-NO and Hp2-2:Hb(II)-NO, respectively ( $k'$ ). From the dependence of  $k'$  on [OH<sup>-</sup>], values of  $h_{\text{OH}^-}$  [ $(4.9 \pm 0.6) \times 10^3$  M<sup>-1</sup> s<sup>-1</sup> and  $(6.79 \pm 0.7) \times 10^3$  M<sup>-1</sup> s<sup>-1</sup>, respectively] and of  $h_{\text{H}_2\text{O}}$  [ $(2.6 \pm 0.3) \times 10^{-3}$  s<sup>-1</sup>] were determined. Values of kinetic and thermodynamic parameters for Hp1-1:Hb(III) and Hp2-2:Hb(III) reductive nitrosylation match well with those of the Hb R-state, which is typical of the  $\alpha\beta$  dimers of Hb bound to Hp.

**Keywords** Ferric human hemoglobin · Human haptoglobin 1-1 · Human haptoglobin 2-2 · Haptoglobin1-1:hemoglobin complex · Haptoglobin2-2:hemoglobin complex · Reductive nitrosylation · Kinetics

## Abbreviations

CCP	Complement control protein
Hb	Hemoglobin
Hb(II)	Ferrous Hb

Hb(III)	Ferric Hb
Hb(II)-NO	Nitrosylated Hb
Hp	Haptoglobin
Hp1-1	Phenotype 1-1 of Hp
Hp2-2	Phenotype 2-2 of Hp
Hp1-1:Hb	Hp1-1:Hb complex
Hp1:Hb(II)	Hp1-1:Hb(II) complex
Hp1-1:Hb(III)	Hp1-1:Hb(III) complex
Hp1-1:Hb(II)-NO	Hp1-1:Hb(II)-NO complex
Hp2-2:Hb	Hp2-2:Hb complex
Hp2-2:Hb(II)	Hp2-2:Hb(II) complex
Hp2-2:Hb(III)	Hp2-2:Hb(III) complex
Hp1-1:Hb(II)-NO	Hp1-1:Hb(II)-NO complex
Mb	Myoglobin
Mb(III)	Ferric Mb
Ngb	Neuroglobin
SP-like domain	Serine protease-like domain

✉ Paolo Ascenzi  
ascenzi@uniroma3.it

<sup>1</sup> Interdepartmental Laboratory of Electron Microscopy, Roma Tre University, Via Della Vasca Navale 79, 00146 Rome, Italy

<sup>2</sup> Department of Sciences, Roma Tre University, Viale Guglielmo Marconi 446, 00146 Rome, Italy

<sup>3</sup> Roma Tre Section, National Institute of Nuclear Physics, Via Della Vasca Navale 84, 00146 Rome, Italy

<sup>4</sup> Department of Clinical Sciences and Translational Medicine, University of Roma "Tor Vergata", Via Montpellier 1, 00133 Rome, Italy

<sup>5</sup> Interuniversity Consortium for the Research on the Chemistry of Metals in Biological Systems, Via Celso Ulpiani 27, 70126 Bari, Italy

## Introduction

Hemoglobin (Hb), the most prominent intracellular protein in blood, carries O<sub>2</sub> in the circulatory system and participates to the metabolism of reactive oxygen and nitrogen species [1–6]. The release of Hb into plasma is a physiological phenomenon, occurring during the hemolysis of senescent erythrocytes and the enucleation of erythroblasts, with potentially severe consequences for health. Moreover, massive intravascular hemolysis, which is accelerated in various autoimmune, infectious (such as malaria), and inherited (such as sickle cell disease) disorders, is a severe pathological complication [1, 7]. To prevent Hb-mediated pathological events, Hb is complexed to haptoglobin (Hp) for clearance by tissue macrophages [7–9].

Hp, the plasma protein with the highest affinity for Hb ( $K_d = 10^{-12}$  M), belongs to the family of acute-phase proteins, is mainly expressed in the liver, and its synthesis is induced by several cytokines during the inflammatory processes [10]. The human Hp gene consists of three structural alleles: Hp1F, Hp1S, and Hp2. The products of the Hp1F and Hp1S alleles differ by only one amino acid, whereas the Hp2 allele is the result of a fusion of the Hp1F and Hp1S alleles giving rise to a longer chain. Hp is expressed as a single polypeptide chain constituted by a complement control protein (CCP) domain and a serine protease- (SP-) like domain. This is proteolytically cleaved into an  $\alpha$  and a  $\beta$  chain covalently linked by a disulfide bond. Hp1 contains a single CCP domain, while Hp2 contains two CCP domains [11]. The three-dimensional structures of porcine [12] and human [13] Hp1-1 in complex with Hb confirmed that the CCP domains display a  $\beta$ -sandwich arrangement. The CCP domains are responsible for a head-to-head dimerization of Hp through an unusual  $\beta$ -strands swap and formation of intermolecular disulfide bonds. The occurrence of the Hp1 and Hp2 alleles in humans gives rise to Hp1-1 dimers (covalently linked by Cys15 residues), Hp1-2 hetero-oligomers and Hp2-2 oligomers (covalently linked by Cys15 and Cys74 residues) [11]. In this latter case, the most abundant oligomer is the tetramer, but trimers and higher order oligomers are also present and have been recently observed at fairly high resolution by cryo-electron microscopy [9].

One  $\alpha\beta$  dimer of Hb binds to each Hp  $\beta$  chain in a 1:1 stoichiometry. Hp makes extensive contacts with the Hb dimer masking the Hb dimer–dimer interface. This is at the root of the high binding affinity between the two proteins and of the ability of Hp to bind only the dimeric form of Hb [9, 13]. The Hp:Hb complexes are subsequently delivered to the reticulo-endothelial system by receptor-mediated endocytosis, CD163 representing the specific receptor for the uptake of the Hp:Hb complex [9, 14].

The Hp:Hb complex has been reported to react with O<sub>2</sub>, CO, and NO [15–17] having properties reminiscent of those of the R quaternary state of the Hb tetramer [12, 13]. To highlight the reactivity properties of the Hp:Hb complex, the reductive nitrosylation of Hp1-1:Hb(III) and Hp2-2:Hb(III) has been investigated between pH 7.5 and 9.5, at  $T = 20.0$  °C. The rate-limiting step of the whole process is represented by the OH<sup>-</sup>/H<sub>2</sub>O-based conversion of Hp1-1:Hb(II)-NO<sup>+</sup> to Hp1-1:Hb(II) and of Hp2-2:Hb(II)-NO<sup>+</sup> to Hp2-2:Hb(II); the formation of the initial Hp:Hb(III)-NO complexes and of the final Hp:Hb(II)-NO adducts being very fast. Kinetics of Hp1-1:Hb(III) and Hp2-2:Hb(III) reductive nitrosylation are similar to those of the Hb R-state, which is typical of the Hp-bound  $\alpha\beta$  dimers of Hb.

## Materials and methods

Human Hp1-1 and Hp2-2 were obtained from Athens Research & Technology, Inc. (Athens, GA, USA). Human oxygenated Hb was prepared as previously reported [18]. The Hp1-1:Hb(II) and Hp2-2:Hb(II) complexes were prepared by mixing oxygenated Hb with Hp1-1 and Hp2-2 at pH 7.3 and 20.0 °C, according to the literature [19]. The dimeric Hp:tetrameric Hb stoichiometry was 1:1. To avoid the presence of free Hb, a 20% excess of Hp1-1 and Hp2-2 was present in all samples; the absence of free Hb was checked by gel electrophoresis [19]. Although deoxygenated Hb does not bind Hp [20, 21], the deoxygenation of the complex formed by either Hp1-1 or Hp2-2 with oxygenated Hb is not followed by any appreciable dissociation [21]. Hp1-1:Hb(III) and Hp2-2:Hb(III) were obtained by adding a few grains of ferricyanide to the protein solutions. Then ferricyanide and by-products were removed by passing the solution through a Sephadex<sup>®</sup> G10 column (Sigma-Aldrich, St. Louis, MO, USA). Hp1-1:Hb(II)-NO and Hp2-2:Hb(II)-NO were obtained by adding a few grains of dithionite and either gaseous NO or the NO solution to the protein solutions. Horse heart myoglobin (Mb) was obtained from Sigma-Aldrich (St. Louis, MO, USA).

Gaseous NO (from Linde Caracciolo S.r.l., Roma, Italy) was purified by flowing through a NaOH column to remove acidic nitrogen oxides. The stock NO solution was prepared anaerobically by keeping, in a closed vessel, the degassed  $5.0 \times 10^{-3}$  M bis-tris propane buffer solution (pH 7.0) under NO at  $P = 760.0$  mm Hg ( $T = 20.0$  °C). The solubility of NO in the aqueous buffered solution is  $2.05 \times 10^{-3}$  M, at  $P = 760.0$  mm Hg and  $T = 20.0$  °C [18]. The concentration of NO in solution was determined, under anaerobic conditions and in the absence of the gaseous phase, by titration of ferrous horse heart Mb, which was monitored by visible absorption spectroscopy [22].

All the other chemicals were obtained from Merck AG (Darmstadt, Germany). All products were of analytical grade and used without purification unless stated.

The reductive nitrosylation of Hp1-1:Hb(III) and Hp2-2:Hb(III) was investigated between pH 7.5 and 9.5 ( $5.0 \times 10^{-2}$  M bis-tris propane buffer), and the nitrosylation of Hp1-1:Hb(II) and Hp2-2:Hb(II) was examined at pH 7.5 and 7.6, respectively. All data were obtained at 20.0 °C.

All the experiments have been carried out with the SFM-20/MOS-200 rapid-mixing stopped-flow apparatus (Bio-Logic Science Instruments, Claix, France); the dead time of the stopped-flow apparatus was ~2 ms, and the observation chamber was 1 cm.

Kinetics and thermodynamics of the reductive nitrosylation of Hp1-1:Hb(III) and Hp2-2:Hb(III) were analyzed in the framework of the minimum reaction mechanism (Scheme 1) [23–35].

Values of the apparent pseudo-first-order rate constant for the reductive nitrosylation of Hp1-1:Hb(III) and Hp2-2:Hb(III) (i.e.,  $k$ ) were obtained by rapid-mixing the Hp1-1:Hb(III) and Hp2-2:Hb(III) solutions (final concentration ranging between  $2.8 \times 10^{-6}$  and  $3.6 \times 10^{-6}$  M) with the NO solution (final concentration,  $4.0 \times 10^{-5}$  to  $1.0 \times 10^{-3}$  M), under anaerobic conditions. No gaseous phase was present. The irreversible reductive nitrosylation of Hp1-1:Hb(III) and Hp2-2:Hb(III) was monitored by single-wavelength stopped-flow spectroscopy between 370 and 450 nm. The amplitude of the time courses was normalized at 395 nm. Values of  $k$  were obtained according to Eq. 1:

$$[\text{Hp:Hb(III)}]_t = [\text{Hp:Hb(III)}]_i \times e^{-k \times t}. \quad (1)$$

However, since only one phase is observed [referable to the cumulative observation of reactions (b–d) and implying a fast pre-equilibrium for reaction (a) (see “Results” and “Discussion”)], the observed rate-limiting pseudo-first-order rate

constant for reductive nitrosylation (i.e.,  $k'$ ) was obtained from the dependence of  $k$  on the NO concentration (ranging between  $4.0 \times 10^{-5}$  and  $1.0 \times 10^{-3}$  M) according to Eq. 2 [23, 24, 36, 37]:

$$k = k' \times [\text{NO}] / (K + [\text{NO}]). \quad (2)$$

Moreover, the dependence of  $k$  on [NO] allowed to determine the equilibrium constant  $K$  for reaction (a).

Values of the apparent second-order rate constant and of the apparent first-order rate constant for the  $\text{OH}^-$ - and  $\text{H}_2\text{O}$ -catalyzed conversion of Hp1-1:(III)- $\text{NO}^+$  to Hp1-1:Hb(II) and of Hp2-2:Hb(III)- $\text{NO}^+$  to Hp2-2:Hb(II) (i.e.,  $h_{\text{H}_2\text{O}}$  and  $h_{\text{OH}^-}$ , respectively; see reaction (c) in Scheme 1) were determined from the dependence of  $k'$  on pH (i.e.,  $[\text{OH}^-]$ ) according to Eq. 3 [23–35]:

$$h' = h_{\text{OH}^-} \times [\text{OH}^-] + h_{\text{H}_2\text{O}}. \quad (3)$$

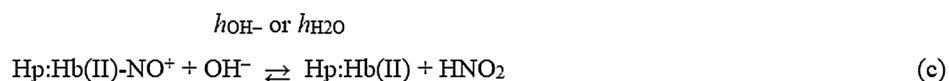
Values of the apparent pseudo-first-order rate constant for Hp1-1:Hb(II) and Hp2-2:Hb(II) nitrosylation of (i.e.,  $l$ ) were obtained by rapid-mixing the Hp1-1:Hb(II) and Hp2-2:Hb(II) solutions (final concentration ranging between  $1.3 \times 10^{-6}$  and  $1.5 \times 10^{-6}$  M) with the NO solution (final concentration, ranging between  $5.0 \times 10^{-6}$  and  $1.5 \times 10^{-5}$  M), under anaerobic conditions. No gaseous phase was present. The nitrosylation of Hp1-1:Hb(II) and Hp2-2:Hb(II) was monitored by single-wavelength stopped-flow spectroscopy at 430 and 415 nm. The amplitude of the time courses was normalized at 430 nm. Values of  $l$  were obtained according to Eq. 4 [38]:

$$[\text{Hp:Hb(II)}]_t = [\text{Hp:Hb(II)}]_i \times e^{-l \times t}. \quad (4)$$

Values of the apparent second-order rate constant for Hp1-1:Hb(II) and Hp2-2:Hb(II) nitrosylation were obtained according to Eq. 5 [38]:

$$l = l_{\text{on}} \times [\text{NO}]. \quad (5)$$

**Scheme 1** Mechanism of reductive nitrosylation of Hp1-1:Hb(III) and Hp2-2:Hb(III)



The results are given as mean values of at least four experiments plus or minus the corresponding standard deviation. All data were analyzed using the MATLAB program (The Math Works Inc., Natick, MA, USA).

## Results

According to Scheme 1, Hp1-1:Hb(III) and Hp2-2:Hb(III) undergo irreversible reductive nitrosylation (i.e., NO-dependent formation of Hp1-1:Hb(II)-NO and Hp2-2:Hb(II)-NO, respectively), between pH 7.5 and 9.5, at  $T=20.0$  °C. In fact, Hp1-1:Hb(II)-NO and Hp2-2:Hb(II)-NO convert to Hp1-1:Hb(II) and Hp2-2:Hb(II), respectively, instead of Hp1-1:Hb(III) and Hp2-2:Hb(III) by pumping off NO. The denitrosylation process of Hp1-1:Hb(II)-NO and Hp2-2:Hb(II)-NO [i.e., the formation of Hp1-1:Hb(II) and Hp2-2:Hb(II)] needs about 6–10 h to be completed; therefore, values of the apparent first-order rate constant for Hp1-1:Hb(II)-NO and Hp2-2:Hb(II)-NO denitrosylation (i.e.,  $k_{\text{off}}$ ; see Scheme 1) are lower than  $2 \times 10^{-4} \text{ s}^{-1}$ .

Upon mixing Hp1-1:Hb(III) and Hp2-2:Hb(III) solutions with the NO solutions, the absorbance changes of Hp1-1:Hb(III) and Hp2-2:Hb(III) nitrosylation [i.e., the formation of Hp1-1:Hb(III)-NO and Hp2-2:Hb(III)-NO] are lost in the dead time of the rapid-mixing stopped-flow apparatus ( $\sim 2$  ms). As a consequence, the absorbance spectra of Hp1-1:Hb(III)-NO and Hp2-2:Hb(III)-NO are observed immediately after mixing, and then, they change gradually to those of Hp1-1:Hb(II)-NO and Hp2-2:Hb(II)-NO. The rate of conversion depending on pH and the NO concentration (see below).

Accordingly, the difference absorbance static spectra of the initial species Hp1-1:Hb(III) and Hp2-2:Hb(III) minus the final species Hp1-1:Hb(II)-NO Hp2-2:Hb(II)-NO, obtained upon adding gaseous NO, differ from the difference absorbance spectra determined after rapid-mixing, since, in the last case, they correspond to those of Hp1-1:Hb(III)-NO minus Hp1-1:Hb(II)-NO and of Hp2-2:Hb(III)-NO minus Hp2-2:Hb(II)-NO (Figs. 1 and 2, panel A). This evidence confirms that the observed time courses (Figs. 1 and 2, panel B) refer to the conversion of Hp1-1:Hb(III)-NO to Hp1-1:Hb(II)-NO and of Hp2-2:Hb(III)-NO to Hp2-2:Hb(II)-NO. As a consequence, unlike for other hemoproteins [25, 27, 28, 30–34], the time courses of Hp1-1:Hb(III) and Hp2-2:Hb(III) reductive nitrosylation turn out to be monophasic for  $96 \pm 5\%$  of their course (Figs. 1 and 2, panel B), corresponding to the reactions (b–d) (see Scheme 1), from which we can obtain the value of  $k$  (see Eq. 1) at different NO concentrations and different pH values. A similar behavior has been already reported for ferric sperm whale Mb [Mb(III)] and human Hb(III) reductive nitrosylation [23, 24].

As shown in Figs. 1 and 2 (panel C), values of the pseudo-first-order rate constant for Hp1-1:Hb(III) and Hp2-2:Hb(III) nitrosylation (i.e.,  $k$ ) do not increase linearly with the NO concentration but tend to level off highlighting the occurrence of a fast pre-equilibrium process followed by a rate-limiting step. As already reported for sperm whale Mb and human Hb reductive nitrosylation [23, 24], the analysis of data shown in Figs. 1 and 2 (panel C) according to Eq. 2 [23, 24, 36, 37] allowed to determine the values of the dissociation equilibrium constant for Hp1-1:Hb(III) and Hp2-2:Hb(III) nitrosylation (i.e.,  $K$ ), and of the first-order rate constant limiting the reductive nitrosylation process (i.e.,  $k'$ ).

As shown in Table 1, values of  $K$  and of  $k'$  for the reductive nitrosylation of Hp1-1:Hb(III) and Hp2-2:Hb(III) are similar over the whole pH range explored (i.e., between pH 7.5 and 9.5). Values of  $K$  for the reductive nitrosylation of Hp1-1:Hb(III) and Hp2-2:Hb(III) are essentially pH-independent; the average values of  $K$  are  $1.1 \times 10^{-4}$  and  $1.3 \times 10^{-4}$  M, respectively. The very fast reaction (a), undetectable by rapid-mixing stopped-flow, has been already observed for the reductive nitrosylation of sperm whale Mb(III) and human Hb(III) [23, 24]. Values of  $K$  allowed to estimate a lower limit for the values of the NO bimolecular association rate constant to Hp1-1:Hb(III) and Hp2-2:Hb(III) (i.e.,  $k_{\text{on}} \geq 3.8 \times 10^6 \text{ M}^{-1} \text{ s}^{-1}$ ) and of the dissociation rate constant for Hp1-1:Hb(III)-NO and Hp2-2:Hb(III)-NO denitrosylation (i.e.,  $k_{\text{off}} \geq 4.4 \times 10^2 \text{ s}^{-1}$ ).

Values of  $k'$  for the reductive nitrosylation Hp1-1:Hb(III) and Hp2-2:Hb(III) increase with pH (Figs. 1 and 2, panels C, D, and Table 1). The values of the rate constants for the  $\text{OH}^-$ - and the  $\text{H}_2\text{O}$ -mediated conversion of Hp:Hb(II)-NO<sup>+</sup> to Hp:Hb(II) (i.e.,  $h_{\text{OH}^-}$  and  $h_{\text{H}_2\text{O}}$ , respectively; see reaction (c) in Scheme 1) were calculated according to Eq. 3. In particular, from the slope of the linear plot of  $k'$  versus  $[\text{OH}^-]$  (Figs. 1 and 2, panel D) the value of the second-order rate constant  $h_{\text{OH}^-}$  was determined. However, since the intercept on the y axis of the linear plot of  $k'$  versus  $[\text{OH}^-]$  (Figs. 1 and 2, panel D) is very small, the value of the pseudo-first-order rate constant  $h_{\text{H}_2\text{O}}$  should be taken as a roughly estimate. As shown in Figs. 1 and 2 (panel D) and in Table 2, values of  $h_{\text{OH}^-}$  and  $h_{\text{H}_2\text{O}}$  are similar for Hp1-1:Hb(II)-NO<sup>+</sup> and Hp2-2:Hb(II)-NO<sup>+</sup> and they match well with those of human Hb [24].

The reaction of Hp1-1:Hb(II) and Hp2-2:Hb(II) with a large concentration of NO (i.e., between  $4.0 \times 10^{-4}$  and  $1.0 \times 10^{-3}$  M) is lost in dead time of the rapid-mixing stopped-flow apparatus ( $\sim 2$  ms). Therefore, values of the apparent second-order rate constant for Hp1-1:Hb(II) and Hp2-2:Hb(II) nitrosylation (i.e.,  $l$ ) were obtained at low NO concentration (i.e., at  $5.0 \times 10^{-6} \text{ M} \leq [\text{NO}] \leq 1.5 \times 10^{-5}$  M). The time courses of Hp1-1:Hb(II) and Hp2-2:Hb(II) nitrosylation are monophasic for more than 87% of their course (Fig. 3, panels A, C). As shown in Fig. 3 (panels B,

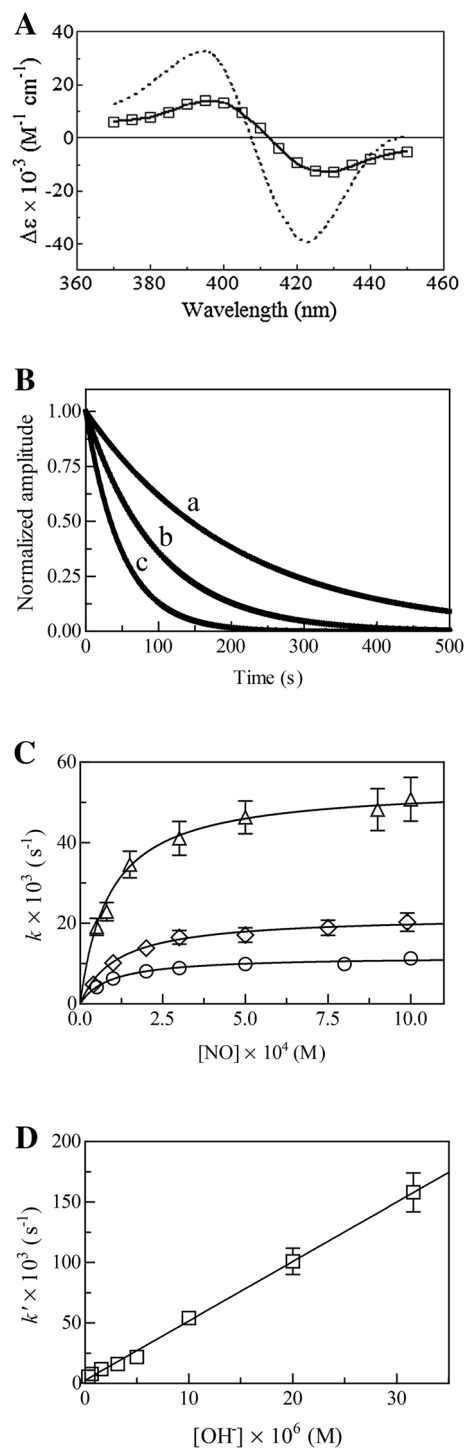
**Fig. 1** Kinetics of Hp1-1:Hb(III) reductive nitrosylation, at 20.0 °C. **A** Difference absorption spectra of Hp1-1:Hb(III) minus Hp1-1:Hb(II)-NO and of Hp1-1:Hb(III)-NO minus Hp1-1:Hb(II)-NO, at pH 8.2 (A). The difference absorption spectrum of Hp1-1:Hb(III) minus Hp1-1:Hb(II)-NO was calculated by subtracting the absolute absorption spectrum of Hp1-1:Hb(II)-NO from that of Hp1-1:Hb(III) (dotted line). The difference absorption spectrum of Hp1-1:Hb(III)-NO minus Hp1-1:Hb(II)-NO was obtained experimentally by rapid-mixing the Hp1-1:Hb(III) and NO solutions (open squares). The difference absorption spectrum of Hp1-1:Hb(III)-NO minus Hp1-1:Hb(II)-NO was calculated by subtracting the absolute absorption spectrum of Hp1-1:Hb(II)-NO from that of Hp1-1:Hb(III)-NO (continuous line). Normalized averaged time courses of Hp1-1:Hb(III) reductive nitrosylation, at pH 8.7 (B). The NO concentration was  $4.0 \times 10^{-5}$  M (trace a),  $1.0 \times 10^{-4}$  M (trace b), and  $9.9 \times 10^{-4}$  M (trace c). The time course analysis according to Eq. 1 allowed the determination of the following values of  $k = (4.8 \pm 0.5) \times 10^{-3} \text{ s}^{-1}$  (trace a),  $(10.2 \pm 1.1) \times 10^{-3} \text{ s}^{-1}$  (trace b), and  $(20.3 \pm 2.3) \times 10^{-3} \text{ s}^{-1}$  (trace c). The concentration of Hp1-1:Hb(III) ranged between  $2.8 \times 10^{-6}$  and  $3.6 \times 10^{-6}$  M. Dependence of the first-order rate constant  $k$  for Hp1-1:Hb(III) reductive nitrosylation on the NO concentration, at pH 8.2 (circles), 8.7 (diamonds), and 9.0 (triangles) (C). The continuous lines were generated from Eq. 2 with the following sets of parameters: pH 8.2,  $K = (0.91 \pm 0.10) \times 10^{-4} \text{ M}$  and  $k' = (11.8 \pm 1.2) \times 10^{-3} \text{ s}^{-1}$ ; pH 8.7,  $K = (1.1 \pm 0.12) \times 10^{-4} \text{ M}$  and  $k' = (21.9 \pm 2.3) \times 10^{-3} \text{ s}^{-1}$ ; and pH 9.0,  $K = (0.88 \pm 0.10) \times 10^{-4} \text{ M}$  and  $k' = (54.1 \pm 5.2) \times 10^{-3} \text{ s}^{-1}$ . Effect of the  $\text{OH}^-$  concentration on the first-order rate constant  $k'$  for Hp1-1:Hb(III) reductive nitrosylation (D). The continuous line was generated from Eq. 3 with the following parameters:  $h_{\text{OH}^-} = (4.9 \pm 0.6) \times 10^3 \text{ M}^{-1} \text{ s}^{-1}$  and  $h_{\text{H}_2\text{O}} = (2.6 \pm 0.3) \times 10^{-3} \text{ s}^{-1}$ . Where not shown, standard deviation is smaller than the symbol. For details, see text

D), values of the pseudo-first-order rate constant for Hp1-1:Hb(II) and Hp2-2:Hb(II) nitrosylation increase linearly with the NO concentration. The analysis of data according to Eq. 4 allowed to determine the values of the apparent second-order rate constant (i.e.,  $l_{\text{on}}$ ; corresponding to the slope of the linear plots) for Hp1-1:Hb(II) and Hp2-2:Hb(II) nitrosylation ( $1.1 \times 10^7$  and  $9.3 \times 10^6 \text{ M}^{-1} \text{ s}^{-1}$ , respectively) (Table 2). The y intercept of the linear plots is close to zero, indicating that NO dissociation from Hp1-1:Hb(II)-NO and Hp2-2:Hb(II)-NO is a very slow process ( $l_{\text{off}} \leq 2 \times 10^{-4} \text{ s}^{-1}$ ; see above) (Table 2). These values agree with those reported for horse heart Mb, sperm whale Mb, and human Hb (Table 2) [29, 38].

## Discussion

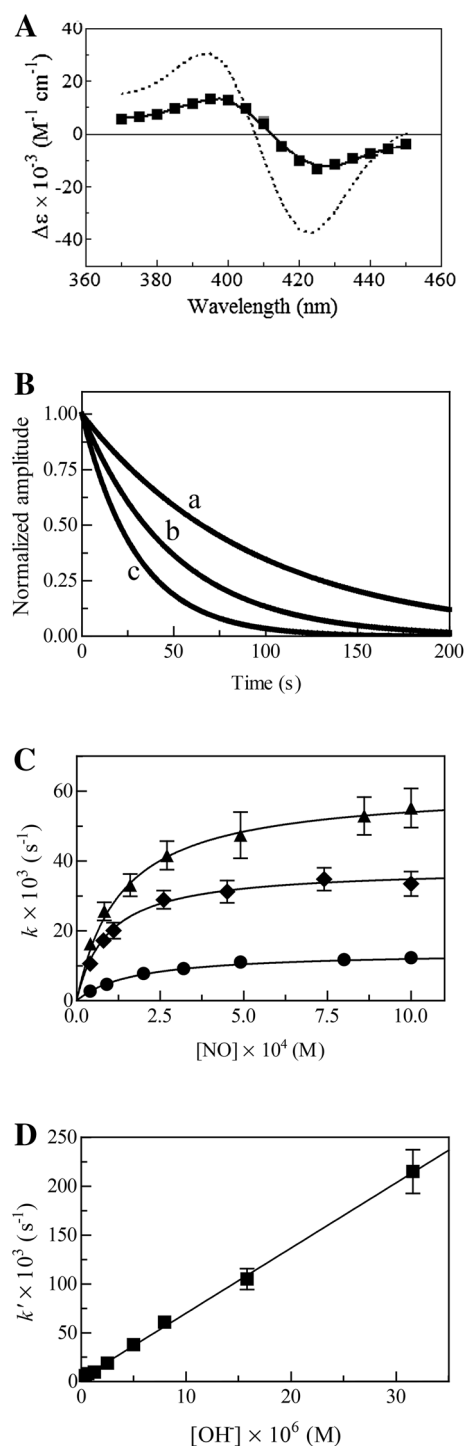
Data here reported allow several considerations, namely:

- (1) The reactivity of dimeric Hp1-1:Hb(III) and Hp2-2:Hb(III) with NO is very high and cannot be determined by rapid-mixing stopped-flow apparatus, resulting much higher than that of ferric horse Mb [29], sperm whale Mb [24], and human neuroglobin (Ngb) [26]. Although the high-spin weak hexa-coordination of the heme-Fe(III) atom by  $\text{H}_2\text{O}$  [13, 39–42] contrib-



utes to a much faster rate in ferric horse Mb [29], sperm whale Mb [24] than in low-spin strong hexa-coordinated hemoproteins (such as human Ngb [26]), the very fast rate observed in Hp1-1:Hb(III) and Hp2-2:Hb(III) (as well likely in tetrameric Hb(III) [24]) must originate from determinants, which are specific of human Hb. As a matter of fact, although NO binding to human Ngb is limited by the cleavage of the labile sixth axial ligand

**Fig. 2** Kinetics of Hp 2-2:Hb(III) reductive nitrosylation, at 20.0 °C. **A** Difference absorption spectra of Hp2-2:Hb(III); minus Hp2-2:Hb(II)-NO: and of Hp2-2:Hb(III)-NO minus Hp2-2:Hb(II)-NO, at pH 8.1 (A). The difference absorption spectrum of Hp2-2:Hb(III) minus Hp2-2:Hb(II)-NO was calculated by subtracting the absolute absorption spectrum of Hp2-2:Hb(II)-NO from that of Hp 2-2:Hb(III) (dotted line). The difference absorption spectrum of Hp2-2:Hb(III)-NO minus Hp2-2:Hb(II)-NO was obtained experimentally by rapidly mixing the Hp2-2:Hb(III) and NO solutions (filled squares). The difference absorption spectrum of Hp 2-2:Hb(III)-NO minus Hp2-2:Hb(II)-NO was calculated by subtracting the absolute absorption spectrum of Hp2-2:Hb(II)-NO from that of Hp2-2:Hb(III)-NO (continuous line). Normalized average time courses of Hp2-2:Hb(III) reductive nitrosylation, at pH 8.7 (B). The NO concentration was  $4.0 \times 10^{-5}$  M (trace a),  $1.1 \times 10^{-4}$  M (trace b), and  $1.0 \times 10^{-3}$  M (trace c). The time course analysis according to Eq. 1 allowed the determination of the following values of  $k' = (10.6 \pm 1.1) \times 10^{-3} \text{ s}^{-1}$  (trace a) ( $20.1 \pm 2.3) \times 10^{-3} \text{ s}^{-1}$  (trace b), and  $(33.5 \pm 3.5) \times 10^{-3} \text{ s}^{-1}$  (trace c). The concentration of Hp2-2:Hb(III) ranged between  $2.8 \times 10^{-6}$  and  $3.6 \times 10^{-6}$  M. Dependence of the first-order rate constant  $k$  for Hp2-2:Hb(III) reductive nitrosylation on the NO concentration (C), at pH 8.4 (circles), 8.7 (diamonds), and 8.9 (triangles). The continuous lines were generated from Eq. 2 with the following sets of parameters: pH 8.4,  $K = (1.7 \pm 0.18) \times 10^{-4} \text{ M}$  and  $k' = (14.0 \pm 1.5) \times 10^{-3} \text{ s}^{-1}$ ; pH 8.7,  $K = (0.92 \pm 0.10) \times 10^{-4} \text{ M}$  and  $k' = (38.0 \pm 3.9) \times 10^{-3} \text{ s}^{-1}$ ; and pH 8.9,  $K = (1.3 \pm 0.12) \times 10^{-4} \text{ M}$  and  $k' = (61.0 \pm 5.8) \times 10^{-3} \text{ s}^{-1}$ . Effect of the  $\text{OH}^-$  concentration on the first-order rate constant  $k'$  for Hp2-2:Hb(III) reductive nitrosylation (D). The continuous line was generated from Eq. 3 with the following parameters:  $h_{\text{OH}^-} = (6.7 \pm 0.7) \times 10^3 \text{ M}^{-1} \text{ s}^{-1}$  and  $h_{\text{H}_2\text{O}} = (2.6 \pm 0.3) \times 10^{-3} \text{ s}^{-1}$ . Where not shown, standard deviation is smaller than the symbol. For details, see text



of the heme-Fe(III) atom (indicated by  $k_{-L}$  in Table 2), preceding the formation of the ferric nitrosylated heme-protein [43], the transient penta-coordinated ferric human Ngb species was never detected, confirming a high intrinsic reactivity of NO for the metal center of this hemoprotein [26]. In any case, the nitrosylation of ferric mammalian heme-proteins does not represent the rate-limiting step (see Table 2).

- (2) Values of  $k_{\text{off}}$  for NO dissociation from ferric nitrosylated horse Mb [29], sperm whale Mb [24], and human Ngb [26] range between  $2.0 \times 10^{-3}$  and  $1.4 \times 10^1 \text{ s}^{-1}$ , reflecting the different structure of the heme distal pocket hosting the heme-bound ligand [39–42]. In the case of Hp1-1:Hb(III)-NO and Hp2-2:Hb(III)-NO, the rate constant must be at least tenfold faster to account for the loss in the dead time of the rapid-mixing stopped-flow apparatus (see above), again confirming a specific structural arrangement of the heme pocket of human Hb, which differs from that of mammalian Mbs and human Ngb [13, 39–42, 44].
- (3) Despite the very different values of  $k_{\text{on}}$  and  $k_{\text{off}}$ , values of  $K$  for ferric heme-protein nitrosylation range between  $7.7 \times 10^{-5}$  to  $2.1 \times 10^{-4} \text{ M}$  (present study and [23, 24, 26, 29]), reflecting the compensation between the association and dissociation kinetic processes (see Table 2).

- (4) The linear dependence of  $h'$  on  $[\text{OH}^-]$  indicates that no additional features appear to be involved in the irreversible reductive nitrosylation of ferric heme-proteins. Moreover, values of  $h_{\text{OH}^-}$  for ferric horse heart Mb [29], sperm whale Mb [24], human Ngb [26], human Hb [24], Hp1-1:Hb(III) (present study), and Hp2-2:Hb(III) (present study) span over four orders of magnitude (Table 2), possibly reflecting the different anion

**Table 1** Values of kinetic parameters for reductive nitrosylation of Hp1-1:Hb(III) and 2-2:Hb(III)

Hp:Hb(III) complex	pH	$K \times 10^4$ (M)	$k' \times 10^3$ (s <sup>-1</sup> )
Hp1-1:Hb(III)	7.5	1.4 ± 0.15	5.6 ± 0.54
Hp1-1:Hb(III)	7.8	1.9 ± 0.20	7.8 ± 0.79
Hp1-1:Hb(III)	8.2	0.91 ± 0.10	11.8 ± 1.2
Hp1-1:Hb(III)	8.5	1.3 ± 0.14	16.0 ± 1.4
Hp1-1:Hb(III)	8.7	1.1 ± 0.12	21.9 ± 2.3
Hp1-1:Hb(III)	9.0	0.88 ± 0.10	54.1 ± 5.2
Hp1-1:Hb(III)	9.3	1.2 ± 0.11	101.0 ± 10.9
Hp1-1:Hb(III)	9.5	0.94 ± 0.10	158.0 ± 16.1
Hp2-2:Hb(III)	7.6	2.1 ± 0.22	6.3 ± 0.67
Hp2-2:Hb(III)	7.8	0.89 ± 0.090	8.1 ± 0.83
Hp2-2:Hb(III)	8.1	1.1 ± 0.13	9.8 ± 0.96
Hp2-2:Hb(III)	8.4	1.7 ± 0.18	19.0 ± 2.0
Hp2-2:Hb(III)	8.7	0.92 ± 0.10	38.0 ± 3.9
Hp2-2:Hb(III)	8.9	1.3 ± 0.12	61.0 ± 5.8
Hp2-2:Hb(III)	9.2	1.8 ± 0.19	105.0 ± 10.7
Hp2-2:Hb(III)	9.5	0.95 ± 0.10	221.0 ± 22.3

$T = 20.0$  °C. Present study

accessibility to the heme pocket and the heme-Fe(III) protein reduction potentials [23, 24, 40–42, 45, 46].

- (5) The rate of the conversion of heme-Fe(II) – NO<sup>+</sup> to heme-Fe(II) + NO<sub>3</sub><sup>-</sup> represents the rate-limiting step of mammalian heme-proteins reductive nitrosylation.

Of note, OH<sup>-</sup> anions catalyze the conversion of heme-Fe(II)-NO<sup>+</sup> to heme-Fe(II) + NO<sub>3</sub><sup>-</sup> more efficiently than H<sub>2</sub>O (i.e.,  $h_{\text{OH}^-} \gg h_{\text{H}_2\text{O}}$ ) (Table 2). This may reflect either the higher affinity of negatively charged ligands for ferric heme-proteins with respect to uncharged compounds and/or the deprotonation rate of the incoming ligand [41, 45, 47].

- (6) Values of  $l_{\text{on}}$  for NO binding to ferrous heme-proteins considered are larger than  $9.3 \times 10^6 \text{ M}^{-1} \text{ s}^{-1}$  (the present study and [29, 38]) (Table 2), indicating that the nitrosylation of the heme-Fe(II) atom does not represent the rate-limiting step of the reductive nitrosylation process.
- (7) Although the geometry of the heme distal pocket of the mammalian heme-proteins considered is quite different [13, 39–42, 44], the very low values of  $l_{\text{off}}$  for NO dissociation from the heme-Fe(II)-NO complexes ( $\leq 1.2 \times 10^{-4} \text{ s}^{-1}$ ) (the present study and [29, 38]; Table 2) reflect the high stability of the ferrous nitrosylated metal centers, possibly representing a case of evolutionary convergence.
- (8) Values of kinetic parameters for human Hb(III) as well as Hp1-1:Hb(III) and Hp2-2:Hb(III) reductive nitrosylation are closely similar reflecting the same structural organization of the ferric Hb tetramer and of the  $\alpha\beta$  Hb dimers bound to Hp; in fact, all these Hb species are frozen in the allosteric R-state [13, 39].

**Table 2** Values of kinetic and thermodynamic parameters for irreversible reductive nitrosylation of ferric mammalian globins

Heme-protein	$k_{\text{L}}$ (s <sup>-1</sup> )	$k_{\text{on}}$ (M <sup>-1</sup> s <sup>-1</sup> )	$k_{\text{off}}$ (s <sup>-1</sup> )	$K$ (M)	$k_{\text{off}}/k_{\text{on}}$ (M)	$h_{\text{OH}^-}$ (M <sup>-1</sup> s <sup>-1</sup> )	$h_{\text{H}_2\text{O}}$ (s <sup>-1</sup> )	$l_{\text{on}}$ (M <sup>-1</sup> s <sup>-1</sup> )	$l_{\text{off}}$ (s <sup>-1</sup> )
Horse heart Mb	–	$6.8 \times 10^{4a}$	$5.2^a$	$1.2 \times 10^{-4a}$	$7.6 \times 10^{-5a}$	$3.9 \times 10^{2b}$	–	$1.6 \times 10^{7a}$	$4.3 \times 10^{-4a}$
Sperm whale Mb	–	$1.9 \times 10^{5c}$	$1.4 \times 10^{1d}$	$7.7 \times 10^{-5c}$	–	$3.2 \times 10^{2e}$	–	$1.7 \times 10^{7f}$	$1.2 \times 10^{-4f}$
Human Ngb fast phase	7.0 <sup>g</sup>	$2.1 \times 10^{1h}$	$2.5 \times 10^{-3h}$	–	$1.2 \times 10^{-4h}$	$\geq 2 \times 10^{6i}$	–	–	–
Human Ngb slow phase	0.6 <sup>g</sup>	2.9 <sup>h</sup>	$2.0 \times 10^{-3h}$	–	$1.9 \times 10^{-4h}$	$\geq 5 \times 10^{5i}$	–	–	–
Human Hb	–	–	–	$8.3 \times 10^{-5j}$	–	$3.2 \times 10^{3k}$	$1.1 \times 10^{-3k}$	$2.4 \times 10^{7f}$	$\sim 3.4 \times 10^{-5f}$
Human Hp1-1:Hb <sup>l</sup>	–	–	–	$1.4 \times 10^{-4}$	–	$4.9 \times 10^3$	$2.6 \times 10^{-3}$	$1.1 \times 10^7$	$< 2 \times 10^{-4}$
Human Hp2-2:Hb <sup>m</sup>	–	–	–	$2.1 \times 10^{-4}$	–	$6.7 \times 10^3$	$2.6 \times 10^{-3}$	$9.3 \times 10^6$	$< 2 \times 10^{-4}$

<sup>a</sup>pH 9.2 and  $T = 20.0$  °C. From [29]

<sup>b</sup> $T = 20.0$  °C. Derived from [29]

<sup>c</sup>pH 8.7; the temperature was not reported. From [23, 24]

<sup>d</sup>pH 8.7; the temperature was not reported. Derived from [23, 24]

<sup>e</sup>The temperature was not reported. From [24]

<sup>f</sup>pH 7.0 and  $T = 20.0$  °C. From [38]

<sup>g</sup>pH 7.0 and  $T = 25.0$  °C. From [43]

<sup>h</sup>pH 7.0 and room temperature. From [26]

<sup>i</sup>Room temperature. Derived from [26]

<sup>j</sup>pH 7.1; the temperature was not reported. From [24]

<sup>k</sup>The temperature was not reported. From [24]

<sup>l</sup>pH 7.5 and  $20.0$  °C. Present study

<sup>m</sup>pH 7.6 and  $20.0$  °C. Present study

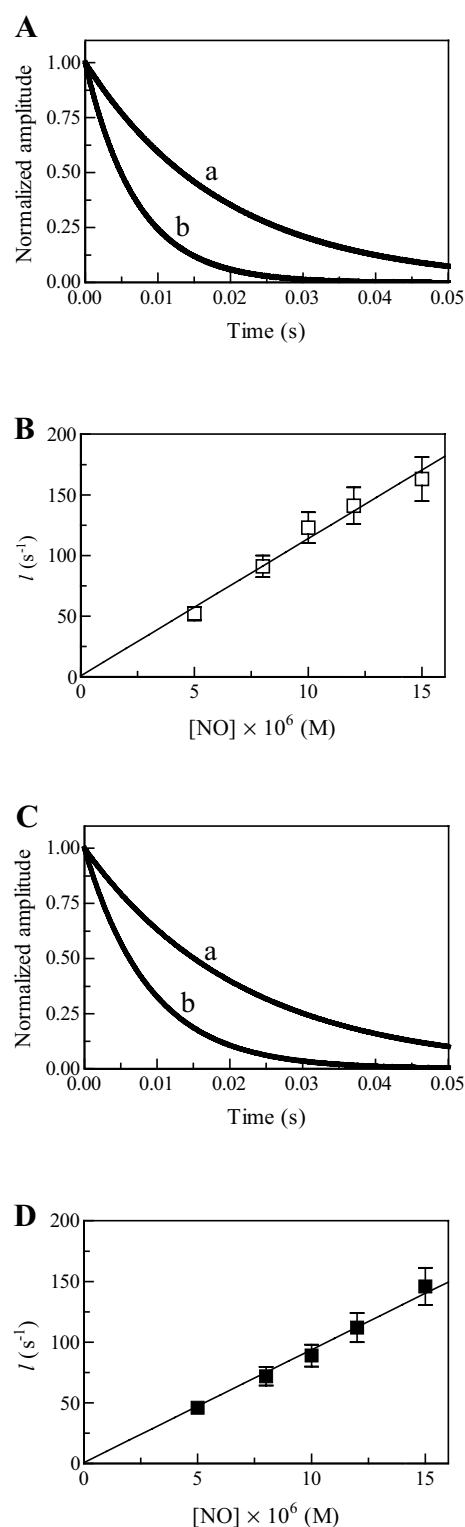
**Fig. 3** Kinetics of Hp1-1:Hb(II) and Hp2-2:Hb(II) nitrosylation, at 20.0 °C. Normalized average time courses of Hp1-1:Hb(II) nitrosylation, at pH 7.5 (A). The NO concentration was  $5.0 \times 10^{-6}$  M (trace a) and  $1.2 \times 10^{-5}$  M (trace b). The time course analysis according to Eq. 4 allowed the determination of the following values of  $l = (5.2 \pm 0.6) \times 10^1 \text{ s}^{-1}$  (trace a) and  $(1.4 \pm 0.2) \times 10^2 \text{ s}^{-1}$  (trace b). The concentration of Hp1-1:Hb(III) was  $1.3 \times 10^{-6}$  M. Dependence of the apparent first-order rate constant  $l$  for Hp1-1:Hb(III) nitrosylation on the NO concentration, at pH 7.5 (B). The continuous line was generated from Eq. 5 with  $l_{\text{on}} = (1.1 \pm 0.1) \times 10^7 \text{ M}^{-1} \text{ s}^{-1}$ . Normalized average time courses of Hp2-2:Hb(II) nitrosylation, at pH 7.6 (C). The NO concentration was  $5.0 \times 10^{-6}$  M (trace a) and  $1.2 \times 10^{-5}$  M (trace b). The time course analysis according to Eq. 4 allowed the determination of the following values of  $l = (4.6 \pm 0.5) \times 10^1 \text{ s}^{-1}$  (trace a) and  $(1.1 \pm 0.1) \times 10^2 \text{ s}^{-1}$  (trace b). The concentration of Hp2-2:Hb(III) was  $1.5 \times 10^{-6}$  M. Dependence of the apparent first-order rate constant  $l$  for Hp2-2:Hb(II) nitrosylation on the NO concentration, at pH 7.6 (D). The continuous line was generated from Eq. 5 with  $l_{\text{on}} = (9.3 \pm 0.9) \times 10^6 \text{ M}^{-1} \text{ s}^{-1}$ . Where not shown, standard deviation is smaller than the symbol. For details, see text

In conclusion, the present results highlight the similar behavior of the reductive nitrosylation of the ferric Hb tetramer and of the  $\alpha\beta$  Hb dimers bound to Hp1-1 and Hp2-2. This finding agrees with kinetics and/or thermodynamics of Hb(II), Hp1-1:Hb(II), and Hp2-2:Hb(II) oxygenation, carbonylation, and nitrosylation as well as of NO detoxification from Hb(II)-O<sub>2</sub>, Hp1-1:Hb(II)-O<sub>2</sub>, and Hp2-2:Hb(II)-O<sub>2</sub> [15–17, 20]. Moreover, values of redox potentials of tetrameric Hb, Hp1-1:Hb and Hp2-2:Hb are strictly comparable [19]. Furthermore, binding of  $\alpha\beta$  Hb dimers to dimeric Hp1-1 and Hp2-2 does not affect the structural properties of the metal centers [12, 13]. Finally, the Hp: $\alpha\beta$  dimer complex formation abrogates the allosteric properties of tetrameric Hb, which correspond to those of the R-state of the tetramer [12, 13]. Interestingly, Hp1-1:Hb and Hp2-2:Hb may display transient functional properties (e.g., NO detoxification) [17], representing a case of “chronosteric effects” [48, 49].

**Acknowledgements** The grant of Excellence Departments, MIUR (Legge 232/2016, Articolo 1, Comma 314-337), is gratefully acknowledged.

## References

- Bunn HF, Forget BG (1986) Hemoglobin: molecular, genetic and clinical aspects. WB Saunders Company, Philadelphia
- Perutz MF (1990) Annu Rev Physiol 52:1–25
- Gow AJ, Luchsinger BP, Pawloski JR, Singel DJ, Stamler JS (1999) Proc Natl Acad Sci USA 96:9027–9032
- Imai K (1999) Nature 401:437–439
- McMahon TJ, Moon RE, Luschinger BP, Carraway MS, Stone AE, Stolp BW, Gow AJ, Pawloski JR, Watke P, Singel DJ, Piantadosi CA, Stamler JS (2002) Nat Med 8:711–717
- Ascenzi P, Brunori M (2016) J Porphyrins Phthalocyanines 20:134–149
- Ascenzi P, Bocedi A, Visca P, Altruda F, Tolosano E, Beringhelli T, Fasano M (2005) IUBMB Life 57:749–759
- Smith A, McCulloh RJ (2015) Front Physiol 6:187
- Andersen CBF, Stødkilde K, Sæderup KL, Kuhlee A, Raunser S, Graversen JH, Moestrup SK (2017) Antioxid Redox Signal 26:814–831
- Wang Y, Kinzie E, Berger FG, Lim SK, Baumann H (2001) Redox Rep 6:379–385





11. Politicelli F, Bocedi A, Minervini G, Ascenzi P (2008) *FEBS J* 275:5648–5656
12. Andersen CB, Torvund-Jensen M, Nielsen MJ, de Oliveira CL, Hersleth HP, Andersen NH, Pedersen JS, Andersen GR, Moestrup SK (2012) *Nature* 489:456–459
13. Stødkilde K, Torvund-Jensen M, Moestrup SK, Andersen CB (2014) *Nat Commun* 5:5487
14. Kristiansen M, Graversen JH, Jacobsen C, Sonne O, Hoffman HJ, Law SK, Moestrup SK (2001) *Nature* 409:198–201
15. Nagel RL, Gibson QH (1966) *J Mol Biol* 22:249–255
16. Chiancone E, Antonini E, Brunori M, Alfsen A, Lavalie F (1973) *Biochem J* 133:205–207
17. Azarov I, He X, Jeffers A, Basu S, Ucer B, Hantgan RR, Levy A, Kim-Shapiro DB (2008) *Nitric Oxide* 18:296–302
18. Antonini E, Brunori M (1971) Hemoglobin and myoglobin in their reactions with ligands. North-Holland Publishing Co, Amsterdam
19. Brunori M, Alfsen A, Saggese U, Antonini E, Wyman J (1968) *J Biol Chem* 243:2950–2954
20. Nagel RL, Whittenberg JB, Ranney HM (1965) *Biochim Biophys Acta* 100:286–289
21. Chiancone E, Wittenberg JB, Wittenberg BA, Antonini E, Wyman J (1966) *Biochim Biophys Acta* 117:379–386
22. Ascenzi P, Brunori M, Pennesi G, Ercolani C, Monacelli F (1987) *J Chem Soc Dalton Trans* 369–371
23. Hoshino M, Ozawa K, Seki H, Ford PC (1993) *J Am Chem Soc* 115:9568–9575
24. Hoshino M, Maeda M, Konishi R, Seki H, Ford PC (1996) *J Am Chem Soc* 118:5702–5707
25. Boffi A, Sarti P, Amiconi G, Chiancone E (2002) *Biophys Chem* 98:209–216
26. Herold S, Fago A, Weber RE, Dewilde S, Moens L (2004) *J Biol Chem* 279:22841–22847
27. Herold S, Puppo A (2005) *J Biol Inorg Chem* 10:946–957
28. Ascenzi P, Bocedi A, Antonini G, Bolognesi M, Fasano M (2007) *FEBS J* 274:551–562
29. Ascenzi P, di Masi A, Gullotta F, Mattu M, Ciaccio C, Coletta M (2010) *Biochem Biophys Res Commun* 393:196–200
30. Ascenzi P, Yu C, di Masi A, Gullotta F, De Sanctis G, Fanali G, Fasano M, Coletta M (2010) *FEBS J* 277:2474–2485
31. Ascenzi P, Pesce A, Nardini M, Bolognesi M, Ciaccio C, Coletta M, Dewilde S (2013) *Biochem Biophys Res Commun* 430:1301–1305
32. Ascenzi P, Marino M, Ciaccio C, Santucci R, Coletta M (2014) *IUBMB Life* 66:438–447
33. Ascenzi P, di Masi A, Tundo GR, Pesce A, Visca P, Coletta M (2014) *PLoS One* 9:e102811
34. Ascenzi P, Bocedi A, Gioia M, Fanali G, Fasano M, Coletta M (2017) *J Inorg Biochem* 177:63–75
35. Ascenzi P, Ciaccio C, De Simone G, Santucci R, Coletta M (2017) *J Porphyrins Phthalocyanines* 21:1–9
36. Antonini E, Ascenzi P, Menegatti E, Guarneri M (1983) *Biopolymers* 22:363–375
37. Bolli A, Ciaccio C, Coletta M, Nardini M, Bolognesi M, Pesce A, Guertin M, Visca P, Ascenzi P (2008) *FEBS J* 275:633–645
38. Moore EG, Gibson QH (1976) *J Biol Chem* 251:2788–2794
39. Perutz MF (1979) *Annu Rev Biochem* 48:327–386
40. Perutz MF (1989) *Trends Biochem Sci* 14:42–44
41. Bolognesi M, Bordo D, Rizzi M, Tarricone C, Ascenzi P (1997) *Prog Biophys Mol Biol* 68:29–68
42. Pesce A, Dewilde S, Nardini M, Moens L, Ascenzi P, Hankeln T, Burmester T, Bolognesi M (2003) *Structure* 11:1087–1095
43. Hamdane D, Kiger L, Dewilde S, Green BN, Pesce A, Uzan J, Burmester T, Hankeln T, Bolognesi M, Moens L, Marden MC (2003) *J Biol Chem* 278:51713–51721
44. Brucker EA, Olson JS, Ikeda-Saito M, Phillips GN Jr (1998) *Proteins* 30:352–356
45. Beetlestone JG, Adeosun OS, Goddard JE, Kushimo JB, Ogunlesi MM, Ogunmola GB, Okonjo KO, Seamonds B (1976) *J Chem Soc Dalton Trans* 1251–1278
46. Miele AE, Santanché S, Travaglini-Allocatelli C, Vallone B, Brunori M, Bellelli A (1999) *J Mol Biol* 290:515–524
47. Giacometti GM, Ascenzi P, Bolognesi M, Brunori M (1981) *J Mol Biol* 146:363–374
48. Antonini E, Ascenzi P, Bolognesi M, Menegatti E, Guarneri M (1983) *J Biol Chem* 258:4676–4678
49. Ascenzi P, Gianni S (2013) *IUBMB Life* 65:836–844